Numerical simulation of damage in glass subjected to static indentation

Jewan Ismail, Fahmi Zairi, Moussa Naït-Abdelaziz, Zitouni Azari

Numerical simulation of damage in glass subjected to static indentation

Jewan Ismail[1], Fahmi Zaïri[1], Moussa Naït-Abdelaziz[1] & Zitouni Azari[2]

[1]*Laboratoire de Mécanique de Lille (UMR CNRS 8107), USTL, Polytech'Lille, Avenue P. Langevin, 59655 Villeneuve d'Ascq Cedex, France*
[2]*Laboratoire de Fiabilité Mécanique de Metz, ENIM, Ile de Saulcy, 57045 Metz Cedex, France*

Abstract:

The present paper is focused on the numerical simulation of a glass plate subjected to static indentation by a spherical indenter. An axisymmetric finite element model of the problem was designed and validated against analytical solutions. A continuum damage mechanics (CDM) based constitutive model with an anisotropic damage tensor was selected and implemented into a finite element code. The numerical results were analysed from the distribution of damage components.

Key-words:

Glass; Indentation; Continuum damage mechanics

1 Introduction

Nowadays, glass is widely used in many engineering applications (civil constructions, vehicles and aircrafts, electronic applications). The most applications of this material have the shape of panels with important areas. Because of the brittleness of glass, the study of the contact problem with external objects is of prime importance.
A particular case of the elastic contact's theory of Hertz is that concerning the contact between a spherical object and a flat surface. When a critical load is achieved, a system of cracks is initiated at the material surface and in its bulk. Significant experimental studies were performed for determining the system of cracks in glasses as well as during the process of indentation that during an impact. As shown in figure 1 in the case of a rigid indenter, the main types of cracks are cone, half-penny, lateral, median and radial cracks (Knight et al., 1977; Cook and Pharr, 1990).

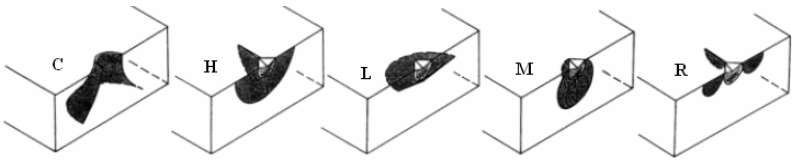

FIG. 1 – Morphologies of different cracks in glass induced by indentation: C) cone, H) half-penny, L) lateral, M) median and R) radial cracks (Cook and Pharr, 1990).

The initiation and propagation of each crack vary according to type of glass (Arora et al., 1979). In particular, for soda-lime glass, the process of fracture regarding the applied load starts firstly by the formation of cone then median cracks when the indenter is still in the stage of loading, though radial and lateral cracks develop later in the stage of unloading. As shown in figure 1, radial and median cracks propagate perpendicularly to the surface; when these two types of cracks intersect each other they form half-penny cracks. While lateral crack propagates in a parallel manner to the surface, and as soon as it intersects with the surface an amount of material is removed. These cracks are generated by principal stresses, i.e. mode I crack opening.
Another deformation observed in glass during an indentation is a permanent deformation named abusively as plastic deformation (Arora et al., 1979). That occurs due either to the significant compaction (densification) of the silicate glass structure or to local shearing (figure 2). The

apparition of this deformation (mode II or sliding mode) is related to shear and compressive hydrostatic stresses.

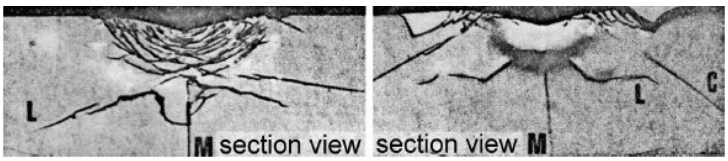

(a) (b)

FIG. 2 – Section views for region beneath an indentation of a) soda-lime glass with deformation by shear flow and b) silica glass with deformation by densification (Arora et al., 1979).

Pioneering works focused on the experimental description of the damage mechanisms in glass. However, the numerical modelling of the damage behaviour of glass during an indentation or an impact is less reported. This modelling is nevertheless essential for a better understanding of damage mechanisms and the design process of glass components. The thermodynamical framework of Continuum Damage Mechanics (CDM) is used in this study. CDM concept was first introduced by Kachanov (1958) and generalized later by Lemaitre and Chaboche (1985). This concept was successfully applied to different classes of materials such as metals, concrete and polymers. Recently, it was applied to glasses by Sun and Khaleel (2004).
In this study, the damage following an indentation on a glass plate by a spherical indenter was analysed by finite element (FE) simulations. For this aim, a CDM based constitutive model was used and implemented into a FE code to describe the damage distribution in the plate. The paper is organized as follows. In section 2, the FE model is detailed. Section 3 is devoted to the description of the CDM model. Section 4 presents the numerical results obtained from FE simulations. Finally, concluding remarks are given in section 5.

2 FE modelling of indentation

FE modelling was used to simulate the indentation process by a rigid sphere in normal contact with a flat plate of glass. The commercial FE code MSC.Marc© was used to carry out the simulations.

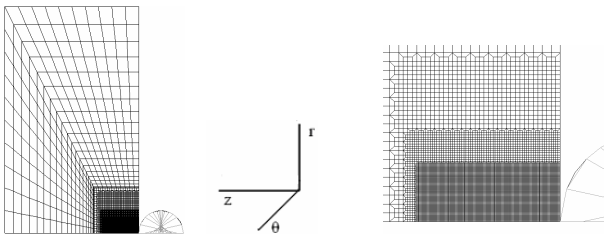

(a) (b)

FIG. 3 – FE model used for the numerical simulations of indentation:
(a) complete mesh and (b) region close to contact.

Due to the axisymmetric character of spherical shaped indentation process, the problem was analysed in a two dimensional axisymmetric cross-sectional model (figure 3). The plate was meshed with a total of 920l axisymmetric four-node isoparametric elements, while the indenter was considered as infinitely rigid. The block of glass was modelled as semi-infinite space in order to the numerical resolution approaches the analytical solutions of the elastic contact's problem of Hertz. No friction between the indenter and the plate was considered. The mechanical properties of the plate used in this study are those of a soda-lime glass. The Young's modulus is taken equal to 72000MPa and the Poisson's ratio to 0.25. Figure 4 illustrates a good

agreement between the analytical solutions of Huber (1904) and numerical results for the principal stresses.

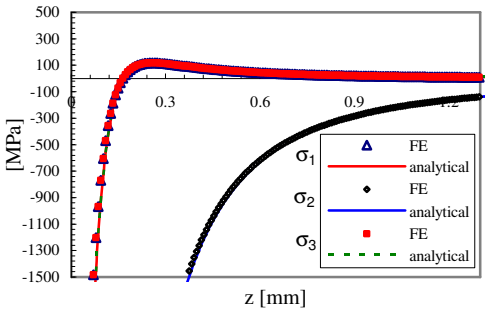

FIG. 4 – Comparison between FE and analytical (Huber, 1904) solutions of the principal stresses for a spherical indenter of 1mm diameter and an applied load of 500N.

Both principal stress σ_1 and σ_2 act in the plan of symmetry, while σ_3 takes action in the direction of θ (figure 3). σ_2 is compressive everywhere within the plate, whereas σ_1 and σ_3 are compressive beneath the contact zone but they become tensile far from this zone. That is illustrated in the contour plots of these stresses shown in figure 5 (Note that white zones in these contour plots are in compression).

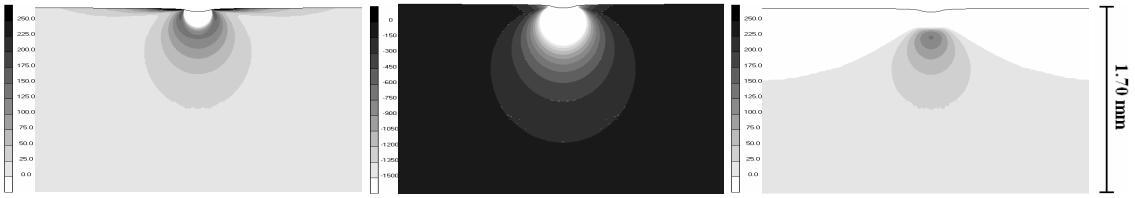

(a) (b) (c)

FIG. 5 – Stresses iso-values obtained by FE simulation in the axisymmetric cross-sectional under an indentation load of 500N by a sphere of 1mm diameter: a) σ_1, b) σ_2, c) σ_3.

3 CDM model

The effect of damage on the deformation process is taken into account by introducing a damage variable into the constitutive equation of the glass material. The damage variable has values between 0.0 (virgin state) and 1.0 (fully damaged state or cracking state). This variable is calculated from a linear evolution law and is introduced into an anisotropic damage matrix D_{ij} which models the material nonlinearity, arising from the deformation process. This anisotropic matrix is added into the constitutive equation of the virgin material which is considered isotropic. The constitutive equation of the glass material is defined by (Sun and Khaleel, 2004):

$$\sigma_{ij} = \left\{ K^e_{ijkl} + K^d_{ijkl} \right\} . \left\{ \varepsilon_{kl} \right\} \tag{1}$$

where K^e_{ijkl} denotes the stiffness matrix for the elastic material and K^d_{ijkl} represents the added damage influence. The full expressions of these tensors components are given by:

$$\begin{aligned} K^e_{ijkl} &= \lambda \delta_{ij} \delta_{kl} + \mu \left(\delta_{ik} \delta_{jl} + \delta_{il} \delta_{kj} \right) \\ K^d_{ijkl} &= C_1 \left(\delta_{ij} D_{kl} + \delta_{kl} D_{ij} \right) + C_2 \left(\delta_{jk} D_{il} + \delta_{il} D_{j_k} \right) \end{aligned} \tag{2}$$

where δ is the Kronecker-delta symbol, λ and μ are the Lame's constants for the glass, C_1 and C_2 are the damage parameters.

3.1 Damage component due to normal principal stresses (mode I)

This component is due to normal principal stresses. Its value is determined according to a simple linear damage evolution law so that, diagonal components of damage are linearly related to the corresponding tensile principal stress components by:

$$D_{ii} = \begin{cases} 0 & \sigma_i \le \sigma_t \\ \dfrac{\sigma_i - \sigma_t}{\sigma_c - \sigma_t} & \sigma_t < \sigma_i < \sigma_c \\ 1 & \sigma_i \ge \sigma_c \end{cases} \tag{3}$$

where σ_c and σ_t are the critical and threshold stresses. σ_t corresponds to the stress below which no damage is visible and σ_c corresponds to the stress above which the material is fully damaged.

3.2 Damage component due to shear stresses (mode II)

As mentioned above, within a zone undergoing a combination state of shear and compressive stresses which exceed certain limits τ_c and τ_t (due to the difficulty of their determination, they are selected to be the same than in mode I (Sun and Khaleel, 2004)), sliding mode (mode II) can be activated. The damage components are also given by a linear evolution law, so in our axisymmetric case they are formulated as a function of shear stress in the plan of symmetry. The general form is:

$$D_{ij} = \begin{cases} 0 & \sigma_{ij} \le \tau_t \quad \text{or} \quad \max(\sigma_i) > 0 \quad i \ne j \\ \dfrac{\sigma_{ij} - \tau_t}{\tau_c - \tau_t} & \tau_t < \sigma_{ij} < \tau_c \quad \text{and} \quad \max(\sigma_i) < 0 \\ 1 & \sigma_{ij} \ge \tau_c \quad \text{and} \quad \max(\sigma_i) < 0 \end{cases} \tag{4}$$

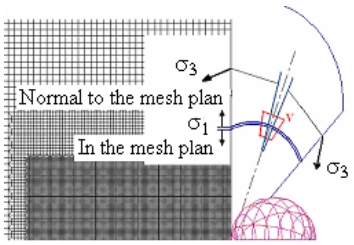

FIG. 6 – Schematic description of σ_1 and σ_3 with corresponding crack propagation.

C_1 and C_2 are determined such as the axial stress equals to zero when the damage component D_{11} approaches 1.0 in a uniaxial tension test. In this study, the parameters values given by Sun and Khaleel (2004) were used: C_1=28800MPa, C_2=-43000MPa, σ_c=216MPa and σ_t=94MPa. The damaged constitutive equations were implemented in the commercial FE code MSC.Marc©.

4 Results and discussion

It is known that each component of principal stresses is responsible of corresponding crack propagation normal to its direction. Since the direction 3 (normal to the mesh plan) is a principal direction, so one can directly expect that principal stress σ_3 contributes to propagate cracks which can be, according to figure 1, median or radial cracks. Moreover on the indented surface, the principal stress σ_1, acting radially as tensile stress, may cause the propagation of a ring

crack which precedes the following development of a cone crack downward. Figure 6 shows a representative volume element V on the indented surface, in which the acting directions of principal stresses σ_1 and σ_3 are defined. The effect of these stresses in the propagation of mode I cracks opening is also shown.

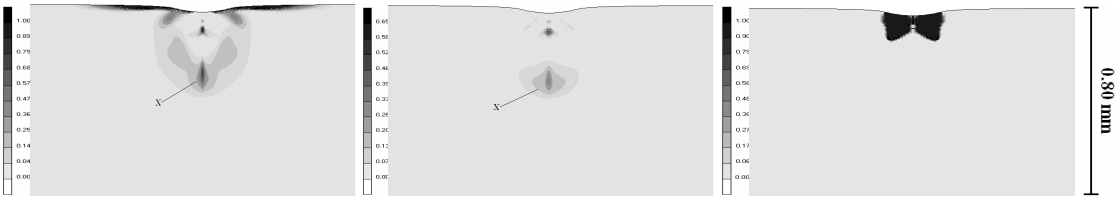

(a) (b) (c)

FIG. 7 – Contour plots of damage components under an indentation load of 500N by a sphere of 1mm diameter: a) D_{11}, b) D_{33}, c) D_{12}.

The iso-value contours of predicted damage components are shown in figure 7. They are obtained in the last increment of calculation, corresponding to a normal static loading of 500N. Concerning the evolution of the damage component D_{11}, it was noticed that as soon as the contact between the sphere and the plate starts, there was a thin damaged zone around the outside edge of the indenter with values less than 1.0. However, with the progress of the indenter in the glass bulk its value increased until 1.0 and it took a circular shape around the sphere. This damaged zone reflects the initiation of a cone crack. Considering the contour plots of the damage components D_{11} and D_{33}, there is an important damaged zone on the symmetry's axis with relatively low damage values. Above this latter zone, occurs another damaged zone on the symmetry's axis which is approximately situated at a distance equal to the radius of contact. This zone exhibits high damage values. It appears because the shear effect (mode II) was taking into account in the modelling. This zone seems to be according to Lawn and Wilshaw (1975) as the bottom of the sheared zone where cracks propagate during the unloading stage because of the mismatch between the sheared zone and the elastic zone surrounding it. According to the damage map D_{12}, we can foresee that this zone is situated just below the bottom of shear damaged zone.

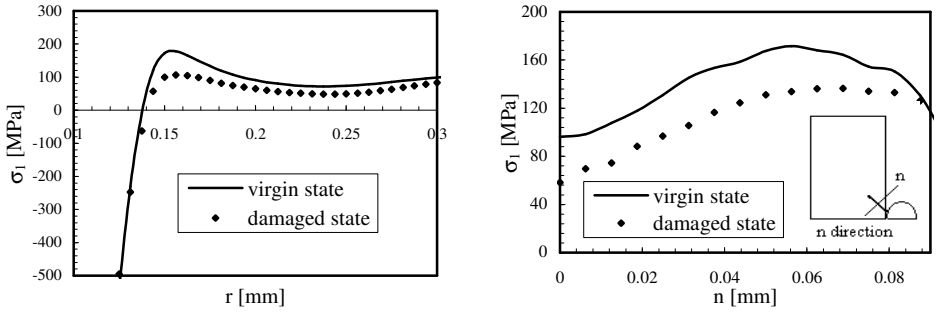

(a) (b)

Fig. 8 – Distribution of maximal principal stress following: a) the radial direction and b) the normal to estimated cone crack direction.

We paid attention on the effect of damage on the distribution of stresses in glass bulk at certain zones after the indentation process. As investigated by Cook and Pharr (1990), the cone crack initiates from the ring crack which seems to be the most damaged zone at the side of the indenter (figure 7a), and it propagates in a direction normal to the maximal principal stress. A radial distribution of this stress at a depth of 0.025mm beneath the indented surface, and another

distribution along a direction normal to estimated cone crack (22°+90°) are plotted in figure 8 for the virgin and damaged cases. A reduction of the maximal principal stress can be clearly seen by taking into account the damage in the modelling.
Also, the distribution of stresses in another region was examined. The damage in this region was registered in both contour plot of D_{11} and D_{33}, which is labelled by X in figure 7. We studied the distribution of all components of principal stresses in this region. Indeed, there is a contribution of more than one principal component which seems to be the responsible of damage in this zone. We plotted in figure 9 the distribution of principal stress σ_3 along two orthogonal paths, close to this region, following radial and axial directions. There is a local effect of predicted damage on this principal stress, which leads to a reduction of its positive values.

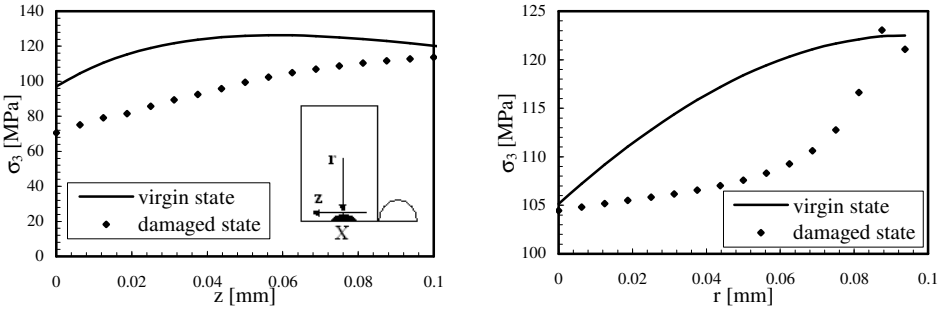

(a) (b)

Fig. 9 – Damage effect on the distribution of principal stress σ_3 in two paths:
a) axial and b) radial, close to the region X.

5 Conclusions

The numerical analysis of a glass plate subjected to static indentation by a spherical indenter was presented. From a CDM based constitutive modelling, the anisotropic damage mechanisms developed in the plate were examined through the principal (mode I) and shear stresses (mode II). As results, many critical zones were highlighted underneath the site of indentation or close to the edge of indenter. The effect of damage on the distribution of stresses around critical zones was studied.
It would be interesting to determine the propagation plan of cracks at every critical zone, since CDM approach does not predict it. Furthermore, it is now of prime importance to conduct our own experimental program to validate the numerical approach adopted in this work.

References

Arora, A., Marshall, D.B., Lawn, B.R. & Swain, M.V. 1979 Indentation deformation/fracture of normal and anomalous glass. *J. Non-Cryst. Solid* **31**, 415-428.

Cook, R.F. & Pharr, G.M. 1990 Direct observation and analysis of indentation cracking in glasses and ceramics. *J. Am. Ceram. Soc.* **73**, 787-817.

Huber, M.T. 1904 Zur theorie der beruhrung fester elasticher korper. *Ann. Phys.* **14**, 153-163.

Kachanov, L.M. 1958 Rupture time under creep conditions. *Izv. Acad. Nauk* **8**, 26-31.

Knight, C.G., Swain, M.V. & Chaudhri, M.M. 1977 Impact of small steel spheres on glass surfaces. *J. Mat. Sci.* **12**, 1573-1586.

Lawn, B. & Wilshaw, R. 1975 Review indentation fracture: principles and applications. *J. Mater. Sci.* **10**, 1049-1081.

Lemaitre, J. & Chaboche, J.L. 1985 Mécanique des matériaux solides. Dunod, Paris.

Sun, X. & Khaleel, M.A. 2004 Modeling of glass fracture damage using continuum damage mechanics – static spherical indentation. *Int. J. Damage Mech.* **13**, 263-285.